JOURNAL OF MATERIALS SCIENCE 37 (2002) 2427–2434

Validation of single-edge V-notch diametral compression fracture toughness test for porous alumina

J. K. CLOBES, D. J. GREEN
Department of Materials Science and Engineering, The Pennsylvania State University, University Park, Pennsylvania 16802, USA

The objectives of this study were to validate a single-edge V-notch diametral compression fracture toughness technique for ceramics. Rounded notches and sharpened "V-notches" were introduced into porous, fine-grained alumina samples, and the fracture toughness results were compared. A theory linking the toughness of the material to the degree of densification fit the fracture toughness results well. The data for the V-notch samples were found to correlate very well with published results for porous alumina. The fracture toughness values were found to be independent of the specimen thickness or notch depth.

1. Introduction

Porous ceramics are becoming increasingly important for applications such as advanced gas and liquid membranes and filters, hot combustion gas "candle" filters, catalyst supports, thermal insulation and thermal barrier coatings, as well as biological applications such as bone substrates [1–5]. These applications often require high strength and/or toughness, among other important properties, therefore accurate mechanical testing techniques are essential for all new or existing materials.

Common mechanical testing techniques such as bend tests are not applicable to small-diameter, thick, cylindrical samples. For cylindrical brittle specimens such as those commonly made in the die-pressing, filter-pressing, or slip-casting of ceramic samples, a very convenient mechanical test is the diametral (or diametrical) compression test. Although strength testing via the diametral compression test is common, the use of diametral compression in fracture *toughness* testing is less prevalent.

The objective of this research is to validate the usefulness and to determine the applicability of the single-edge V-notch diametral compression fracture toughness test by testing porous, fine-grained alumina. Different aspects of the test are scrutinized, such as the necessity for a sharp notch-tip, the effect of notch depth and the effect of sample thickness.

2. Background

Some researchers have used diametral compression for toughness testing with success [6–17], but the notching techniques can be problematic depending on the sample dimensions and level of porosity. For example, internal notches and chevron notches require precise and somewhat difficult machining, and chevron through-notches cannot easily be applied to thick samples. For porous ceramics, indentation methods may not be very applicable, as the cracks and the stress field are not well-defined. A single-edge notch is, however, relatively simple to machine, is applicable to small-diameter or thick samples, and can be made large compared to the microstructural features. In addition, a "V-notch" can easily be machined into the bottom of the single-edge notch, thus enhancing the stress concentrations at the bottom of the 'V' to create a sharp crack front.

The diametral compression test involves the loading of a cylindrical specimen along its diameter such that tensile stresses are created perpendicular to the load. It is an attractive test in that it allows brittle materials to be tested in tension without loading and gripping difficulties and the specimen shape is easy to produce. The stress state is both compressive and tensile. For line loading at the contact points, the horizontal tensile stress, σ_x, is constant along the loaded diameter and is given by [18]

$$\sigma_x = \frac{2P_y}{\pi\, \mathrm{d}t} \tag{1}$$

where P_y is the load, d the specimen diameter, and t the thickness (cylinder height). The most important stress state for brittle failure is the *tensile* stress state, which is given by [18]

$$\sigma_x = \frac{2P_y}{\pi\, \mathrm{d}t} - \frac{2P_y}{\pi t} \times \left\{ \frac{x^2(R-y)}{[x^2+(R-y)^2]^2} + \frac{x^2(R+y)}{[x^2+(R+y)^2]^2} \right\} \tag{2}$$

where R is the specimen radius and x and y are the Cartesian coordinate positions, with $x = 0$ and $y = 0$ at the sample center. Evaluation of this equation shows

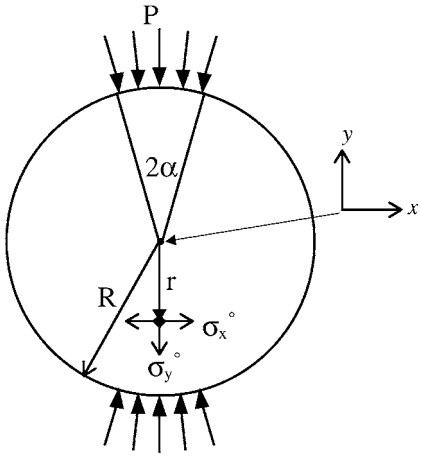

Figure 1 The diametral compression test under distributed load.

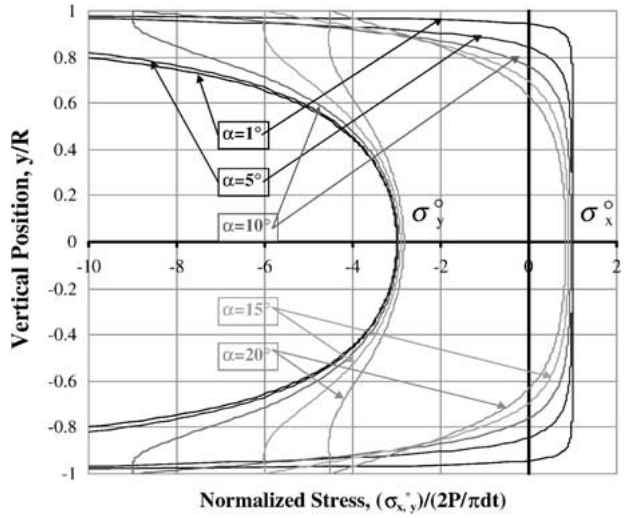

Figure 2 Normalized stress at $x = 0$ as a function of position along the y-axis for load-distribution half-angles, α. Horizontal stresses are given as σ_x°; vertical stresses are σ_y°.

that the edge of the specimen is subjected to a very low stress except near the contact points. This implies that edge flaws away from the loading points are unlikely to be a source of failure.

Plastic deformation and crushing of the sample near the contact points is of great concern. To minimize the contact stresses, bearing strips can be used to distribute the load over a portion of the surface. These cushions are placed between the platens and the contact points before testing. Fig. 1 is a schematic diagram of load distribution. The load is spread out over a certain arc length (corresponding to the angle 2α) of the cylinder, and the contact pressure is thereby lowered, helping to ensure that failure occurs internally. The effect of the bearing strips on the stress components has been discussed elsewhere [19]. The stress distribution along the diametral plane (where $x = 0$) has been derived by Hondros [20]. With respect to Fig. 1,

$$\sigma_x^\circ = \frac{2P_y}{\pi\, \mathrm{d}t\alpha}\left\{\frac{[1-(\bar{r})^2]\sin 2\alpha}{1-2(\bar{r})^2\cos 2\alpha+(\bar{r})^4} - \tan^{-1}\left[\frac{1+(\bar{r})^2}{1-(\bar{r})^2}\tan\alpha\right]\right\} \tag{3}$$

$$\sigma_y^\circ = -\frac{2P_y}{\pi\, \mathrm{d}t\alpha}\left\{\frac{[1-(\bar{r})^2]\sin 2\alpha}{1-2(\bar{r})^2\cos 2\alpha+(\bar{r})^4} + \tan^{-1}\left[\frac{1+(\bar{r})^2}{1-(\bar{r})^2}\tan\alpha\right]\right\} \tag{4}$$

where $\bar{r}$ is the ratio of the radial position over the total radius ($\bar{r} = r/R$). The largest horizontal tensile stress is found at the center of the disk (where $r = 0$), and is of magnitude [18]

$$\sigma_{\text{tens}} = \frac{2P_y}{\pi\, \mathrm{d}t}\left(\frac{\sin 2\alpha - \alpha}{\alpha}\right) \tag{5}$$

When α is very small, $\sin 2\alpha \approx 2\alpha$, and the equation simplifies to Equation 1, as expected for line loading.

Equations 3 and 4 are plotted in Fig. 2. This graph shows the variance of the stresses along the y-axis for a variety of half-angles, α. A few important features can be found. First, the application of load distribution produces *horizontal compressive* stresses near the contact points. Second, the compressive stresses *at the loading points* (both vertical (σ_y) and horizontal (σ_x)) decrease rapidly with increasing α. Third, as expected from Equation 5, the horizontal tensile stress near the center of the disk decreases as α increases.

Fracture toughness testing with a single-edge notch has been performed previously. In this method a notch is introduced along the loading diameter on one of the faces of the specimens. Szendi-Horvath [21, 22] introduced this method to find the toughness of "soda glass," Perspex ("plexiglass"), and coal. The results of this experiment for the glass showed that even though the notch bottom of the glass was not sharp, the results agreed with that of a double-torsion test. Szendi-Horvath attributed this to cracks originating "at sharp scratches or imperfections in the bottom of the groove", and noticed that the crack initiated at the bottom of the notch. The experiment also showed that the specimen size had no effect on the measured toughness, nor did the depth of the grooves. It was also determined that the groove does not require great accuracy in positioning at the center of the diameter. Singh and Pathan [23] also investigated the single-edge notch diametral compression test on five rock types: sandstone, siltstone, coal, basalt, and granite. Their results agreed with Szendi-Horvath's in that the measured toughness was independent of crack length, but to the contrary, they found that fracture toughness depended on the thickness to diameter ratio.

For a semi-infinite plate with an edge-crack subjected to tension, the toughness is given by

$$K_{\text{IC}} = \sigma_{\text{f}} Y\sqrt{c} = 1.12\sigma_{\text{f}}\sqrt{\pi c} \tag{6}$$

where σ_{f} is the failure stress and c is the notch or crack depth. Combining Equations 5 and 6,

$$K_{\text{IC}} = \frac{2.24}{\sqrt{\pi}}\frac{P_{\text{f}}\sqrt{c}}{\mathrm{d}t}\frac{(\sin 2\alpha - \alpha)}{\alpha} \tag{7}$$

where P_{f} is the failure load.

In the toughness testing of materials, it is important to have a sharp "crack" front. Damani *et al.* [24] found that "the notch width must be of the order of the size of the relevant microstructural or machining-induced defects (e.g. large pores and weak grain boundaries)" to produce accurate toughness measurements. Pre-cracking of the specimens can be performed, but is usually impractical because it can be difficult to induce a precrack in some ceramics, and it is often difficult to measure the precrack length in opaque ceramics.

A "sharp" notch can be introduced with a "V-notch." To make a perfect V-notch, one would need a perfectly "V"-shaped wheel. V-edged diamond wheels have been used previously to notch a variety of ceramics [25, 26], where the V-notch tip radii ranged from about 8 to 33 μm. It was found that smaller tip radii yielded slightly smaller toughness values, presumably due to the higher stress concentrations produced by the notch. Other methods are available to sharpen an existing notch. The method used in the current study was to sharpen an existing notch using a razor blade sprinkled with diamond paste. This procedure has been performed before with success [27–29].

As the current work is concerned with the effect of porosity on fracture toughness, it is useful to compare the results to existing theories. Various theories exist to relate the fracture toughness to the porosity of ceramics [30]. For example, Lam *et al.* [31] have shown the fracture toughness can be given as

$$K_{\mathrm{IC}} = K_{\mathrm{IC0}}\left(\frac{\rho - \rho_{\mathrm{g}}}{1 - \rho_{\mathrm{g}}}\right) = K_{\mathrm{IC0}}\left(1 - \frac{P}{P_{\mathrm{g}}}\right) \quad (8)$$

where ρ is the relative density, P is the porosity, the subscript 0 signifies a property of the fully-dense body, the subscript g signifies a property of the green body and the quantity $(1 - P/P_{\mathrm{g}})$ is the *degree of densification*, i.e., the 'fraction' the material has densified since the green state.

Hardy and Green [32] modified this theory by taking into account the fracture toughness of the body just before the onset of densification, assuming that bodies with porosity P_{g} will have a fracture toughness greater than zero. To incorporate this idea, a term was added to Equation 8:

$$\left(\frac{K_{\mathrm{IC}} - K'_{\mathrm{IC}}}{K_{\mathrm{IC0}} - K'_{\mathrm{IC}}}\right) = \left(1 - \frac{P}{P_{\mathrm{g}}}\right) \quad (9)$$

where K'_{IC} is the fracture toughness at the onset of densification.

3. Experimental procedure

A set of approximately 130 samples was slip cast from a fine alumina powder (A16-SG, Alcoa Industrial Chemicals, Bauxite, AR). The particle size of this powder ranges from about 0.12 to 20 μm, with median particle size 0.4 μm and specific surface area of $\sim$9.5 m^2/g [33]. Alumina/water slurries with 50 volume% solids loading were made by milling a mixture of powder, deionized water, and polyelectrolyte dispersant (Duramax D-3007, Rohm and Haas, Philadelphia, PA) for about 24–48 hours in a high-density polyethylene bottle.

TABLE I Typical batch amounts for a 40 mL slurry

Component	Content (g)
Alumina	78.93
Deionized water	19.84
Dispersant D-3007	0.82
Binder B-1000	0.38

Shear rate tests run on the slurry showed the viscosity to be about 25 mPa · s (25 cP) at this point. A water-miscible binder (Duramax B-1000, Rohm and Haas, Philadelphia, PA) with a low glass transition temperature (-26°C) was mixed in after milling. An example of the typical batch amounts for a 40-mL volume of slurry is given in Table I.

After binder addition, the slurry was transferred to a glass beaker, stirred slowly on a magnetic stirrer to prevent coagulation, and de-aired under vacuum. Plastic eye-droppers were used to transfer the slurry into teflon rings (1.27 cm inside diameter, 2.54 cm height) set on top of flat, relatively smooth gypsum molds. Care was used to prevent air from being trapped within the transferred slurry. The slurry was filled to a depth of about 1.3 cm (1/2 in.). The samples were allowed to cast for up to 24 hours (at least until hardened), then allowed to air dry within the rings before removal. No cracking was observed in the samples due to drying.

The thickness of the dry samples was reduced to a desired height by grinding the top surfaces of the samples on silicon carbide paper, grit sizes 240, 320, and then 600. The bottom surface was also "polished" using 600-grit paper. At this point excess debris was wiped off of each specimen, and the green diameter and thickness was measured. The organics were burned out of the specimens by ramping a furnace (model CSF1200, Labline/Carbolite, Barnstead/Thermolyne, Dubuque, IA) to 700°C. After burnout the mass of the samples was measured. The "green bulk density" was now obtained from the dimensions and the mass after burnout.

The samples were fired at 1090°C to impart sufficient strength, then were surface-ground using a 10.2 cm (4 in.) diameter, 1.3 cm (1/2 in.) wide diamond-coated wheel (Diamond Devices Inc., Auburn, CA) attached to a precision dicing machine ("Micro-Matic", Micromech Mfg. Corp., Rahway, NJ). This process allowed the sample size to be reduced to any desired thickness, and also made the surface to be notched flat and relatively smooth. The samples were cleaned in water and acetone after surface grinding with the help of a sonic bath (model 2200, Branson Ultrasonics Corp., Danbury, CT).

Firing of the samples was performed in either the same furnace used for the organics pyrolysis or a high-temperature (up to 1700°C) furnace (model 51314, Lindberg, Watertown, WI). The heating profiles were 5°C/min to the firing temperature (1100 to 1650°C), with a 2-hour hold. After firing, the dimensions and mass were taken for each sample to determine the fired bulk density.

Notches with depth of approximately 1/4 of the thickness (or height) of the cylindrical specimens were

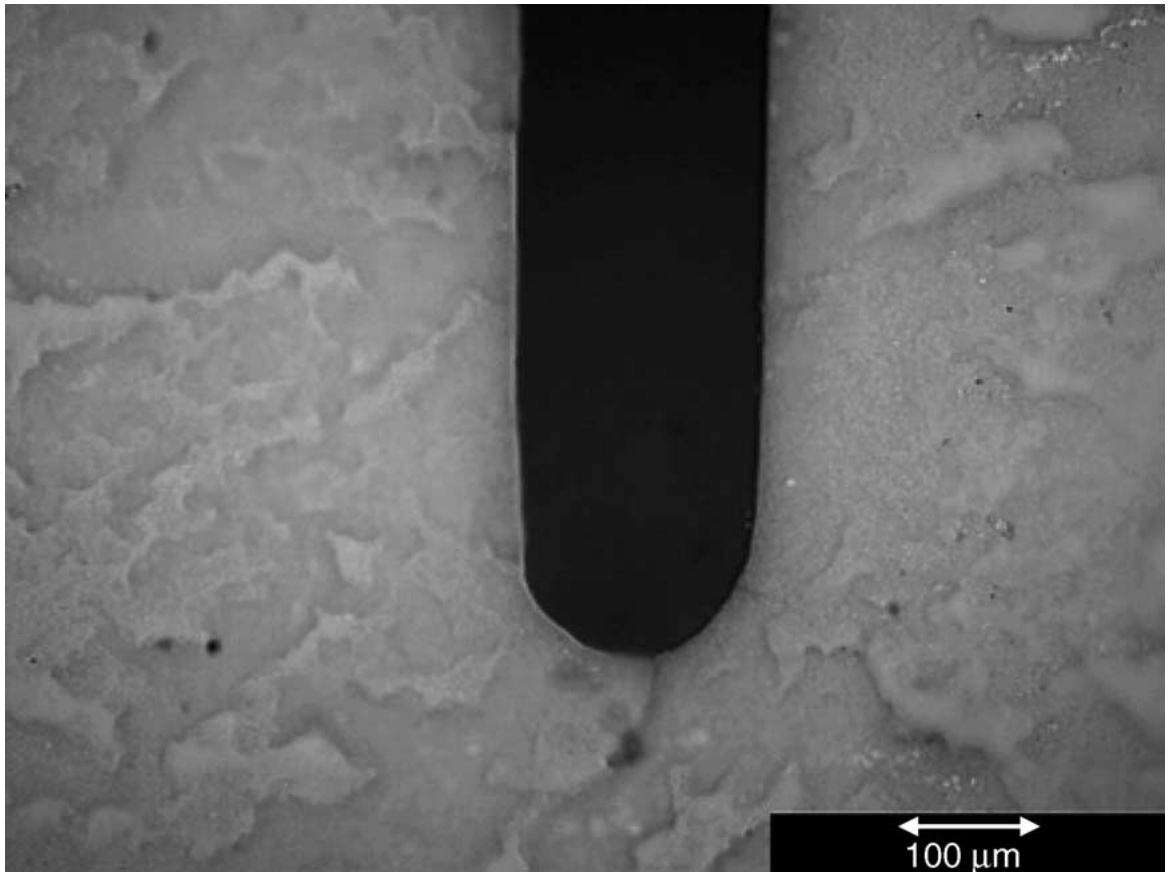

Figure 3 Photograph of an "unmodified" notch in a sample fired at 1300°C.

cut using an alignment jig (described elsewhere [19]), diamond-coated wafering blades (numbers 11-4254 and 11-4253, Buehler, Lake Bluff, IL), and the precision dicing machine. The smaller blade was 7.6 cm (3 in.) in diameter by 0.15 mm (6 mils) thick and was used for selected samples fired at 1100–1400°C. These notches tended to be rounded at the bottom, as shown in Fig. 3. Once cut, these notches were not modified any further, and therefore are called "unmodified" for the purpose of this report. The larger blade was 10.2 cm (4 in.) in diameter by 0.3 mm (12 mils) thick and was used to notch selected samples, fired at 1100–1650°C, prior to "V-notching." After notching, water and acetone washes were again performed using the sonic bath. To remove the final residue left after washing, one more heating step was employed in a furnace to 750°C, with a 20–30 minute hold. Determination of the mass before and after this last heating step showed that a slight, but significant, amount of impurity was burned out. After the heating step, Archimedes' density measurements were performed on each of the samples using kerosene (K10-4, Fisher Scientific Inc., Pittsburgh, PA) as the liquid medium.

"V-notching" of many selected samples was performed using razor blades ("American Line", American Safety Razor Co., Staunton, VA) to enhance the sharpness of the notch tip of selected samples. First the more robust single-edge blade of thickness 0.30 mm (0.012 in.) was coated with 2–4 μm diamond paste (Kay Industrial Diamond Corp., Deerfield Beach, FL) and was pushed back and forth inside the notch to start a sharper groove. The thinner 0.225 mm (0.009 in.) blade was then coated with the diamond paste and used to further enhance the sharpness of the cut. The V-notching process was more time-consuming for the higher-density samples fired at 1300°C and above. The paste was cleaned out of the groove using acetone and the sonic bath. The notch depth was measured using an optical microscope and a Vernier eyepiece as the average of the total groove depth at both ends of the notch. The V-notches looked similar to the one shown in Fig. 4.

A mechanical testing machine (model 4202, Instron, Canton, MA) fitted with a 10 kg load cell was used to obtain the diametral compression results. A spherical bearing was used to ensure alignment of the loading platens. The samples were aligned as shown schematically in Fig. 5. The crosshead speed of the mechanical tester was set between 0.07 and 0.10 mm/min for the notched samples, such that each specimen failed after 3 to 7 minutes. Bearing strips (two strips of manila folders) were used as stress "cushions" between the platens and the samples. Upon testing, the sample first indented into the strips, leaving about a 1 to 3 mm-wide impression in the strips (depending upon the final force at breakage). The width of these impressions were measured after the test so that the angle α (Fig. 1) could be determined. The test was stopped at the first sign of failure, usually the audible sound of a crack and a sudden decrease in the load. At this point the sample was 'fractured,' however, the small indent in the bearing strips, together with the horizontal compressive stresses near the load points, was enough to support the cracked halves from separating. Therefore, each run had to be

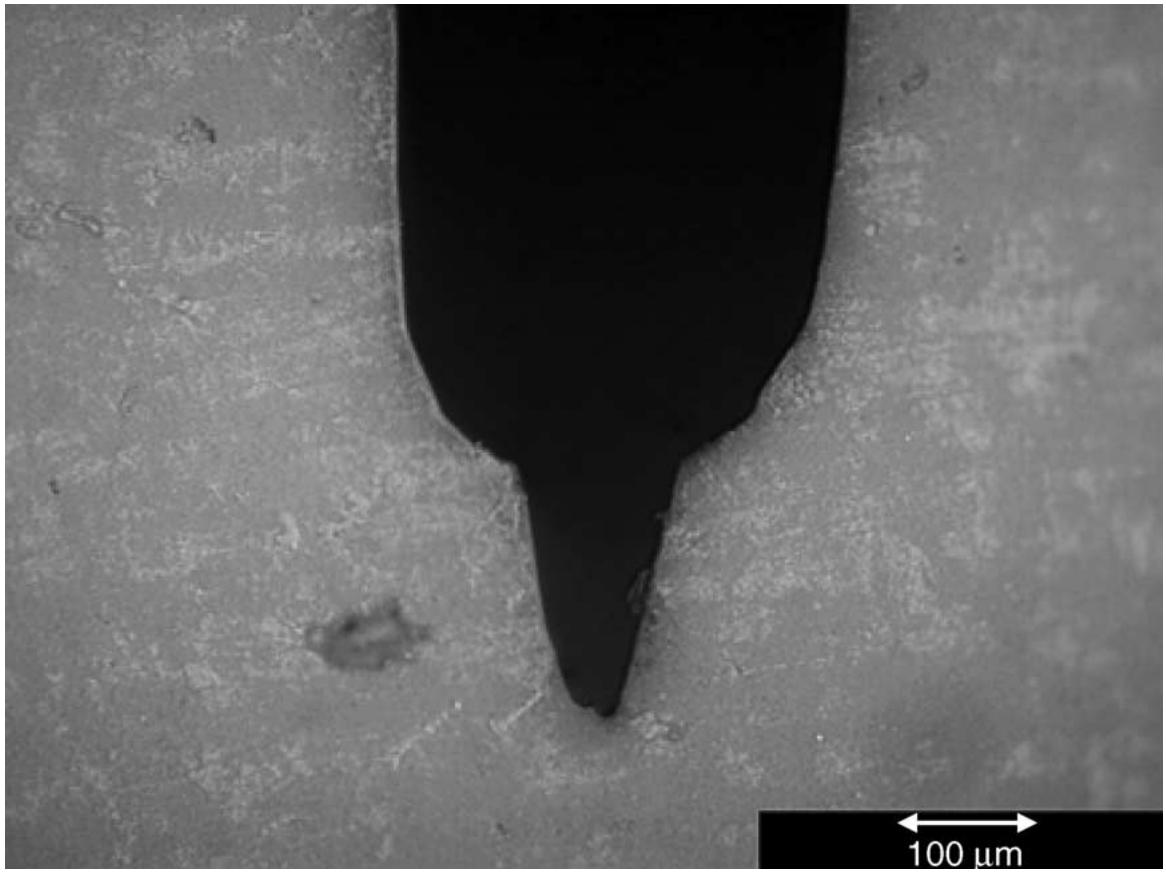

Figure 4 Photograph of a "V-notch" in a sample fired at 1300°C.

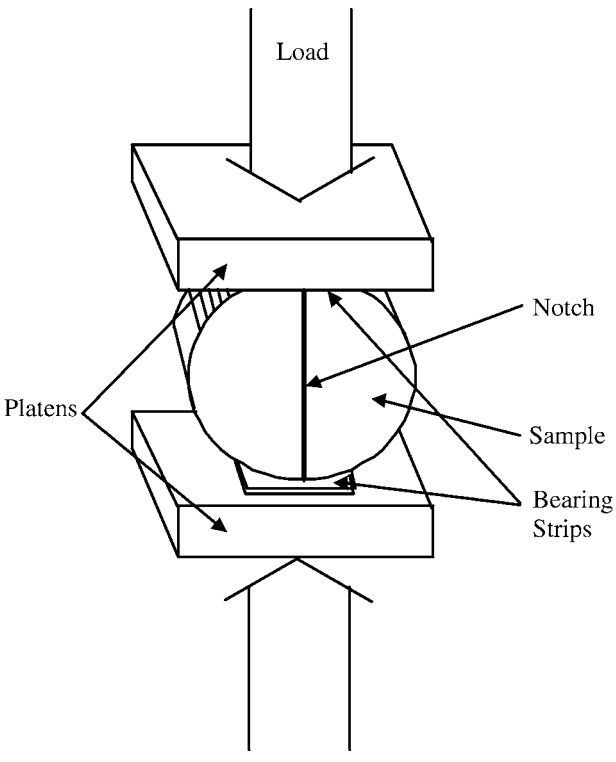

Figure 5 Schematic of the specimen/platen portion of the diametral compression test.

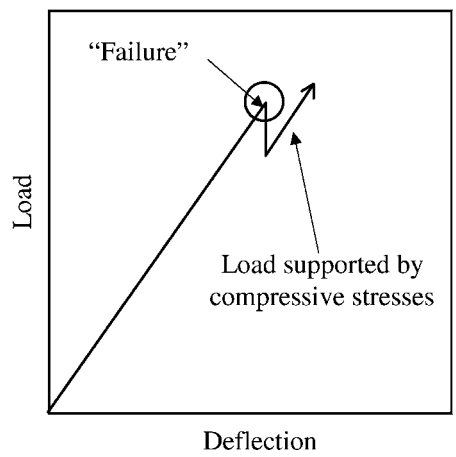

Figure 6 Schematic of a load/deflection curve during the mechanical testing of a specimen.

observed closely to ensure that the load did not extend beyond the initial breaking point. Using this method, the fracture load was found for each sample. A schematic of a load/deflection curve found for this test is shown in Fig. 6. The test was ended when the failure crack was observed.

The fracture surfaces of a selection of the samples were observed using a scanning electron microscope, or SEM, (Model XL 20, Philips Electronics N. V., Eindhoven, The Netherlands). A calibrated optical microscope (Model BX60M, Olympus Optical Co., Ltd., Tokyo, Japan) was used to estimate notch-tip radii.

4. Results and discussion

4.1. Dimensional and densification analysis

The samples produced for these experiments had a reasonably high green density that ranged from 2.56

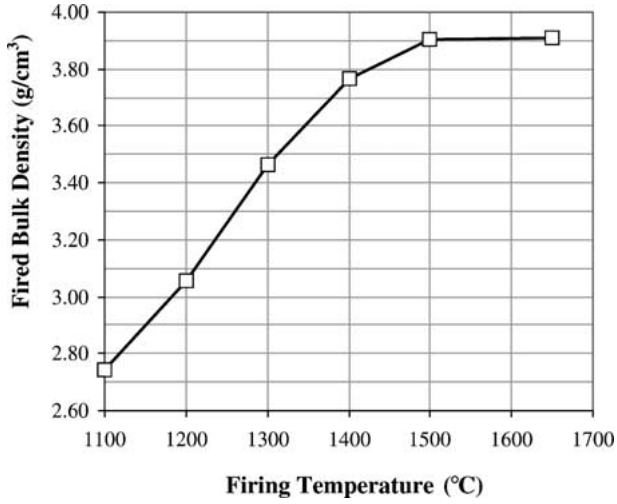

Figure 7 Fired bulk density as a function of firing temperature.

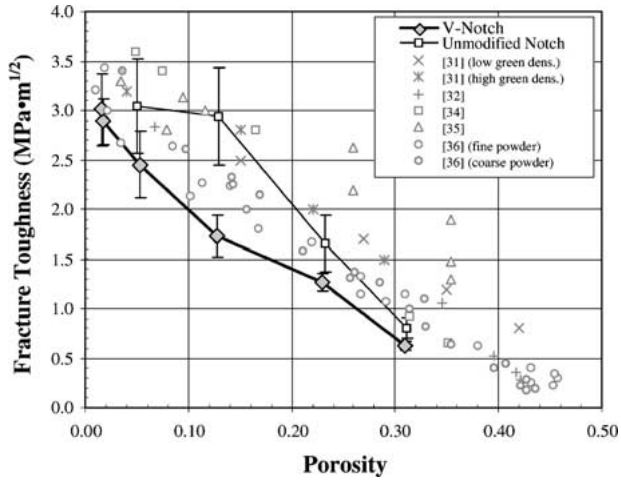

Figure 8 Fracture toughness of the V-notched and unmodified notch specimens versus porosity. The error bars are plus or minus one standard deviation.

to 2.65 g/cm^3. This corresponds to about 64.4 to 66.6% relative density. The average green density was 2.60 g/cm^3 (65.4% relative density), with a standard deviation of $\pm$0.03 g/cm^3 ($\pm$0.7% relative density). The compacts were fired at a variety of temperatures ranging from 1100 to 1650°C. As expected, the fired density increased as the firing temperature increased. The relationship between fired bulk density and the firing temperature is shown in Fig. 7. The density values had standard deviations of approximately $\pm$0.005 to 0.026 g/cm^3. The porosity fraction was determined from the density values using a theoretical density for the alumina of 3.98 g/cm^3. The Archimedes' density results showed that the porosity was almost entirely "open," or interconnected for compacts fired at 1300°C and below, and almost entirely "closed" for compacts fired at 1400°C and above.

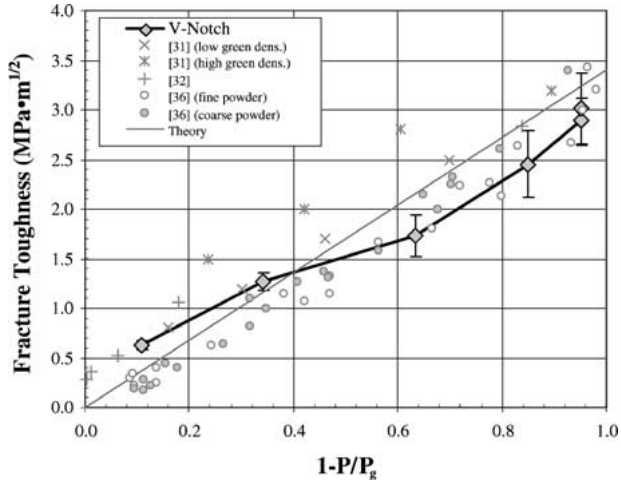

Figure 9 Fracture toughness of the V-notched and unmodified notch specimens versus the degree of densification. The error bars are plus or minus one standard deviation.

4.2. Fracture toughness of unmodified notch and V-notch specimens

The fracture toughness was calculated using Equation 7, assuming the initial crack depth is the notch depth. The angle α was determined geometrically from the width of the impression on the bearing strips, and was typically about 10–25°. About 5–14 samples per firing temperature were tested and averaged to obtain the results.

The results for fracture toughness as a function of porosity are shown in Fig. 8 together with other published results on the fracture toughness of fine-grained alumina [31, 32, 34–36]. The difference between the V-notch and the unmodified notch results is substantial. For every data point that can be compared, at a given porosity level the measured fracture toughness is substantially lower for the V-notched samples. These results seem to indicate that the extra sharpness of the V-notch increases the stress concentration at the bottom of the notch, thus inducing crack initiation and subsequent failure at lower stresses [26]. However, comparing the V-notch results to the previously published alumina toughness data, the fracture toughness measured by the diametral compression single-edge V-notch technique is relatively low for the entire data set. This can be explained by considering that the green densities of all of these samples were generally quite high, and have not been accounted for in Fig. 8. The 65.4% relative density of the samples in this experiment is significantly higher than the 50 and 62% for Lam *et al.* [31], the 57.8% green density for Hardy and Green [32], and the 50 and 52% for Ostrowski and Rödel [36] (no green density data was mentioned in the other two publications). The use of Equation 8 normalizes the data to the green density (which is assumed to have a fracture toughness of zero), thereby bringing all the data sets together regardless of their green density.

Fig. 9 is a plot of the V-notch data for this theory, and it shows that the V-notch fracture toughness data not only follows the theory well, it also correlates well with the previously published data (with the exception of one of the data sets from [31]). For high porosity, extrapolation of the data to $P = P_g$, allows $K_{IC,init}$ (the fracture toughness of the body just upon densification) in Equation 9 to be estimated as 0.28 MPa$\sqrt{}$m.

The difference between the results of the unmodified notch and that of the V-notch must be the effect of

the notch-root radius. Comparison of the difference in values between the two experimental data sets suggests that the notch-root radius does not have a great effect on the fracture toughness measurement of high porosity (low density) ceramics. This can be reasoned from the idea that porosity at the bottom of the notch may be acting as stress concentrations.

The notch-root radius is an important feature of the V-notch. While opinions differ as to what the critical notch radius (ρ_C) is, where radii smaller than the certain ρ_C will yield the "true" measured fracture toughness, it appears that ρ_C is material-dependent. Claussen *et al.* stated that the critical notch radius was about 50 μm for all ceramics, and that it increased for porous materials [34]. Kübler stated that the critical notch radius is about 30 μm [29], while Nishida *et al.* showed that above a notch radius of 10 μm, the fracture toughness of dense alumina apparently begins to increase [27].

Estimations of the notch-root radii showed that samples fired at 1300°C and below ($P > 12\%$) were easily V-notched to a root radius of 10–25 μm or less. For samples fired at temperatures 1400°C and higher, the V-notch was more difficult to make "sharp." The notch radii for samples with $P < 7\%$ tended to be between 20 and 50 μm, which is near or in the range for valid radii. For the unmodified notch samples, the average notch radius was about 70–80 μm, which is out of the range of "valid radii" as described above. This is expected to be the most important reason for the relatively high fracture toughness values shown by the unmodified notch samples.

4.3. Validity of the testing technique

The diametral compression V-notch testing technique was found to be a useful test, however, there are some provisions (a more detailed discussion of the sources of error in the test is given in [19]). The notch must be cut within about 5% of the diameter to avoid a large (>5%) reduction in stress at the notch tip. The testing platens must be perpendicular to the notch within about 5° or 6.5° to prevent stress reductions of greater than 3%, or 5%, respectively. Considerations also need to be made for the accurate measurement of the notch depth, especially in samples with very shallow notches where the errors would be more significant. In general, the larger the notch depth the smaller the potential error. Subcritical crack growth in the material must also be taken into account for tests performed over relatively long time periods. Thus, it is suggested that tests are performed at rapid loading rates to minimize these effects.

4.4. The effect of notch depth on the fracture toughness test

Szendi-Horvath [21] and Singh and Pathon [23] found that the fracture toughness results from the single-edge notch diametral compression test were independent of initial crack-length. For thoroughness, it was decided to verify those results using the V-notch technique.

A set of 30 samples was fired to 1200°C. The samples were subsequently divided randomly into five groups, six specimens per group. Each group was notched to a different depth: 0.1, 0.2, 0.3, 0.4, and 0.5 times the thickness. The results of this experiment are presented in Table II and as expected, showed no dependence on notch depth.

TABLE II Average fracture toughness for fine-grained alumina (fired at 1200°C) with varying notch depth

(Notch depth)/ (thickness), c/t	Fracture toughness ($MPa \cdot m^{1/2}$)	Standard deviation $\pm$ ($MPa \cdot m^{1/2}$)
0.1	1.07	0.10
0.2	1.04	0.11
0.3	1.15	0.07
0.4	1.20	0.20
0.5	1.15	0.07

4.5. The effect of specimen thickness on the fracture toughness test

Szendi-Horvath [21] tested the effect of specimen size on the fracture toughness and found that a variance in specimen size (diameter or thickness) had no noticeable effect (as expected from Equation 1). However, Singh and Pathon [23] found that the fracture toughness is dependent upon the thickness-to-diameter ratio of the specimens. In their study of five types of rocks, they discovered that the fracture toughness slightly increased with increasing thickness/diameter (t/d) ratio until it reached a plateau around $t/d = 0.8$.

Samples were made with unfired thicknesses of 3.75, 4.5, and 5.5 mm. They were fired at 1100–1400°C, and notched with V-notches to 1/4 depth of their fired thickness. The average fracture toughness was found for each separate data set. The results of this study are presented in Fig. 10. Note that these are the same data as given in Fig. 9, except that here the sets are "ungrouped" to subdivide among the different sample thicknesses. As shown in Fig. 10, there is no significant difference between any of the common sets (samples fired at the same temperature and tested with the same type of notch).

4.6. Fracture surface microscopy

SEM (scanning electron microscope) micrographs of the fracture surfaces showed a transition from complete intergranular to a large amount of intragranular

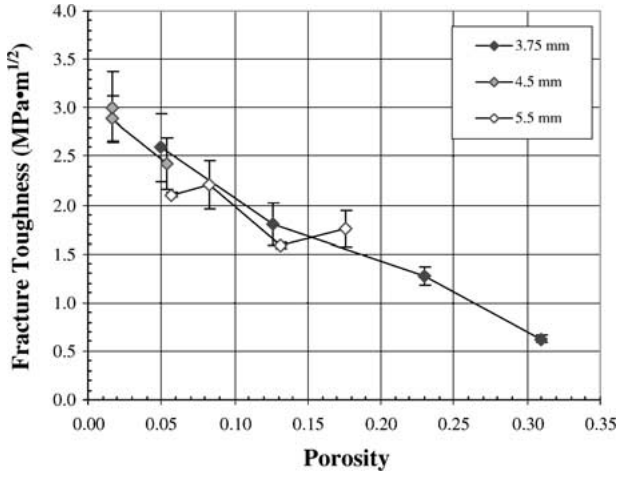

Figure 10 Fracture toughness results for samples of different thickness (measured in the green state). The error bars are plus or minus one standard deviation.

fracture from 1300°C to 1500°C. Lower sintering temperatures (below 1300°C) led to low fired density with limited grain growth. As the sintering temperature was increased, the grain size ranges increased from 0.1–1 μm at 1300°C to 0.5–3 μm at 1500 and 1–15 μm at 1650°C.

5. Summary and conclusions

The single-edge V-notch diametral compression toughness test was found to be applicable to the fracture toughness measurement of porous alumina. It was found that the fracture toughness was directly proportional to the degree of densification of the material.

The data for the V-notched specimens correlated well with the previously published data from other authors for the fracture toughness of porous alumina. The V-notch has to be sufficiently sharp such that the notch-tip radius is very small, approximately less than about 30 μm, to ensure that the stress concentrations at the bottom of the notch are large enough to make the groove act as a sharp crack. The V-notches in this study had tip radii of about 10–30 μm. The fracture toughness of the porous alumina did not vary with notch depth or specimen thickness.

It is concluded that the V-notch diametral compression technique is a valid fracture toughness test for porous alumina. It is expected to be applicable to other ceramics, regardless of porosity. The test is particularly useful and convenient for small-diameter cylindrical specimens, when other testing techniques are more difficult to perform.

Acknowledgments

This work was based in part on the thesis submitted by J. K. Clobes for the M. S. degree in Materials Science and Engineering, The Pennsylvania State University, University Park, PA, 2001. It was financially supported by the National Science Foundation under Grant 97-04281.

References

1. M. A. ALVIN, T. E. LIPPERT and J. E. LANE, *Am. Cer. Soc. Bull.* **70**(9) (1991) 1491.
2. J. F. ZIEVERS and P. EGGERSTEDT, *ibid.* **70**(1) (1991) 108.
3. K. K. CHAN and A. M. BROWNSTEIN, *ibid.* **70**(4) (1991) 703.
4. J. CHARPIN, A. J. BURGGRAAF and L. COT, *Ind. Cer.* **11**(2) (1991) 84.
5. R. W. RICE, in "Porosity of Ceramics" (Marcel Dekker, 1998) p. 475.
6. H. AWAJI and S. SATO, *J. Eng. Mater. Technol.* **100** (1978) 175.
7. C. ATKINSON, R. E. SMELSER and J. SANCHEZ, *Int. J. Fract.* **18**(4) (1982) 279.
8. S. Y. YAREMA, G. S. IVANITSKAYA, A. L. MAISTRENKO and A. I. ZBOROMIRSKII, *Probl. Prochn.* **16**(8) (1984) 1121.
9. D. MIESS and G. RAI, *Mater. Sci. Eng.* A **209** (1996) 270.
10. T. TANG, *J. Test. Eval.* **22**(5) (1994) 401.
11. D. K. SHETTY, A. R. ROSENFIELD and W. H. DUCKWORTH, *J. Amer. Ceram. Soc.* **68**(12) (1985) C-325.
12. *Idem.*, *Eng. Fract. Mech.* **26**(6) (1987) 825.
13. D. SINGH and D. K. SHETTY, *J. Mater. Sci.* **23** (1988) 968.
14. *Idem.*, *J. Amer. Ceram. Soc.* **72**(1) (1989) 78.
15. D. K. SHETTY, A. R. ROSENFIELD and W. H. DUCKWORTH, *ibid.* **69**(6) (1986) 437.
16. Z. XIAOLI, W. CHONGMIN and Z. HONGTU, *J. Mater. Sci. Lett.* **6** (1987) 1459.
17. K. KENDALL and R. D. GREGORY, *J. Mater. Sci.* **22** (1987) 4514.
18. M. K. FAHAD, *ibid.* **31** (1996) 3723.
19. J. K. CLOBES, M. S. Thesis, The Pennsylvania State University, University Park, PA, 2001.
20. G. HONDROS, *Aust. J. Appl. Sci.* **10** (1959) 243.
21. G. SZENDI-HORVATH, *Eng. Fract. Mech.* **13** (1980) 955.
22. *Idem.*, *Aust. J. Coal Min. Technol. Res.* **2** (1982) 51.
23. R. N. SINGH and A. G. PATHAN, *Min. Sci. Technol.* **6** (1988) 179.
24. R. DAMANI, R. GSTREIN and R. DANZER, *J. Eur. Ceram. Soc.* **16** (1996) 695.
25. H. AWAJI, T. WATANABE and Y. SAKAIDA, *Ceram. Int.* **18** (1992) 11.
26. M. MIZUNO and H. OKUDA, *J. Amer. Ceram. Soc.* **78**(7) (1995) 1793.
27. T. NISHIDA, Y. HANAKI and G. PEZZOTTI, *ibid.* **77**(2) (1994) 606.
28. J. KÜBLER, *Ceram. Eng. Sci. Proc.* **18**(4) (1997) 155.
29. *Idem.*, *ibid.* **20**(3) (1999) 495.
30. R. W. RICE, in "Porosity of Ceramics" (Marcel Dekker, Inc., 1998) p. 168.
31. D. C. LAM, F. F. LANGE and A. G. EVANS, *J. Amer. Ceram. Soc.* **77**(8) (1994) 2113.
32. D. HARDY and D. J. GREEN, *J. Eur. Ceram. Soc.* **15** (1995) 769.
33. "Reactive and Calcined Aluminas for Refractories and Ceramics" (Alcoa World Chemicals, USA/0047-R02/0700, 2001) p. 1.
34. N. CLAUSSEN, R. PABST and C. P. LAHMANN, *Proc. Brit. Cer. Soc.* **25** (1975) 139.
35. C. C. WU and R. W. RICE, *Ceram. Eng. Sci. Proc.* **6**(7/8) (1985) 977.
36. T. OSTROWSKI and J. RÖDEL, *J. Amer. Ceram. Soc.* **82**(11) (1999) 3080.

Received 8 August 2001
and accepted 24 January 2002